Supplement of Geosci. Model Dev., 13, 2511–2532, 2020
https://doi.org/10.5194/gmd-13-2511-2020-supplement


Geoscientific Model Development
Open Access
EGU

*Supplement of*

# Investigating the sensitivity to resolving aerosol interactions in downscaling regional model experiments with WRFv3.8.1 over Europe

**Vasileios Pavlidis et al.**

*Correspondence to:* Vasileios Pavlidis (vapavlid@physics.auth.gr)

# Supplement

*Table S1. Domain averaged precipitation difference (mm/day) and relative difference (%) from CON. For all experiments and seasons. Where stated, for simulation ARCI the above quantities are also calculated against ACI (ARCI-ACI) in order to assess the implementation of aerosol-radiation interactions in the Thompson aerosol-cloud interacting cloud microphysics.*

| | DJF | | MAM | | JJA | | SON | |
|---|---|---|---|---|---|---|---|---|
| | mm/day | relative % | mm/day | relative % | mm/day | relative % | mm/day | relative % |
| ARI_T | 0,00 | 0 | -0,08 | -4 | -0,08 | -5 | 0,04 | 2 |
| ARI_Mv1 | 0,00 | 0 | -0,05 | -2 | -0,02 | -2 | 0,00 | 0 |
| ARI_Mv1urban | -0,05 | -2 | -0,24 | -13 | -0,21 | -14 | -0,06 | -2 |
| ARI_Mv1full | -0,01 | 0 | -0,01 | 0 | 0,00 | 0 | 0,06 | 3 |
| ARI_MC | 0,01 | 0 | -0,09 | -5 | -0,03 | -2 | 0,02 | 1 |
| ARCI-ACI | -0,04 | -1 | 0,02 | 1 | -0,03 | -2 | -0,13 | -5 |
| | | | | | | | | |
| ACI | -0,04 | -2 | -0,05 | -3 | 0,00 | 0 | 0,07 | 3 |
| ARCI | -0,08 | -3 | -0,03 | -2 | -0,04 | -2 | -0,06 | -2 |

*Table S2. Relative difference (%) from control CON for shortwave radiation (Rsds), direct normalized irradiance (DNI) and diffuse radiation at the surface (DIF). Where stated, for simulation ARCI the above quantities are also calculated against ACI (ARCI-ACI) in order to assess the implementation of aerosol-radiation interactions in the Thompson aerosol-cloud interacting cloud microphysics. For all simulations and seasons.*

| | DJF | | | MAM | | | JJA | | | SON | | |
|---|---|---|---|---|---|---|---|---|---|---|---|---|
| | Rsds | DNI | DIF | Rsds | DNI | DIF | Rsds | DNI | DIF | Rsds | DNI | DIF |
| ARI_T | -5 | -30 | 7 | -4 | -22 | 12 | -7 | -27 | 36 | -8 | -31 | 16 |
| ARI_Mv1 | -5 | -33 | 8 | -5 | -29 | 17 | -6 | -30 | 38 | -7 | -34 | 18 |
| ARI_Mv1urban | -11 | -33 | -3 | -12 | -29 | 0 | -13 | -29 | 12 | -16 | -37 | 1 |
| ARI_Mv1full | -4 | -31 | 9 | -5 | -28 | 17 | -7 | -29 | 37 | -6 | -33 | 18 |
| ARI_MC | -3 | -26 | 7 | -5 | -27 | 15 | -6 | -29 | 35 | -7 | -29 | 15 |
| ARCI-ACI | -2 | -20 | 6 | -4 | -23 | 12 | -6 | -25 | 26 | -3 | -18 | 14 |
| | | | | | | | | | | | | |
| ACI | 7 | 8 | 7 | 7 | 9 | 5 | 9 | 11 | 6 | 8 | 6 | 7 |
| ARCI | 5 | -14 | 13 | 2 | -16 | 17 | 2 | -17 | 31 | 5 | -14 | 21 |

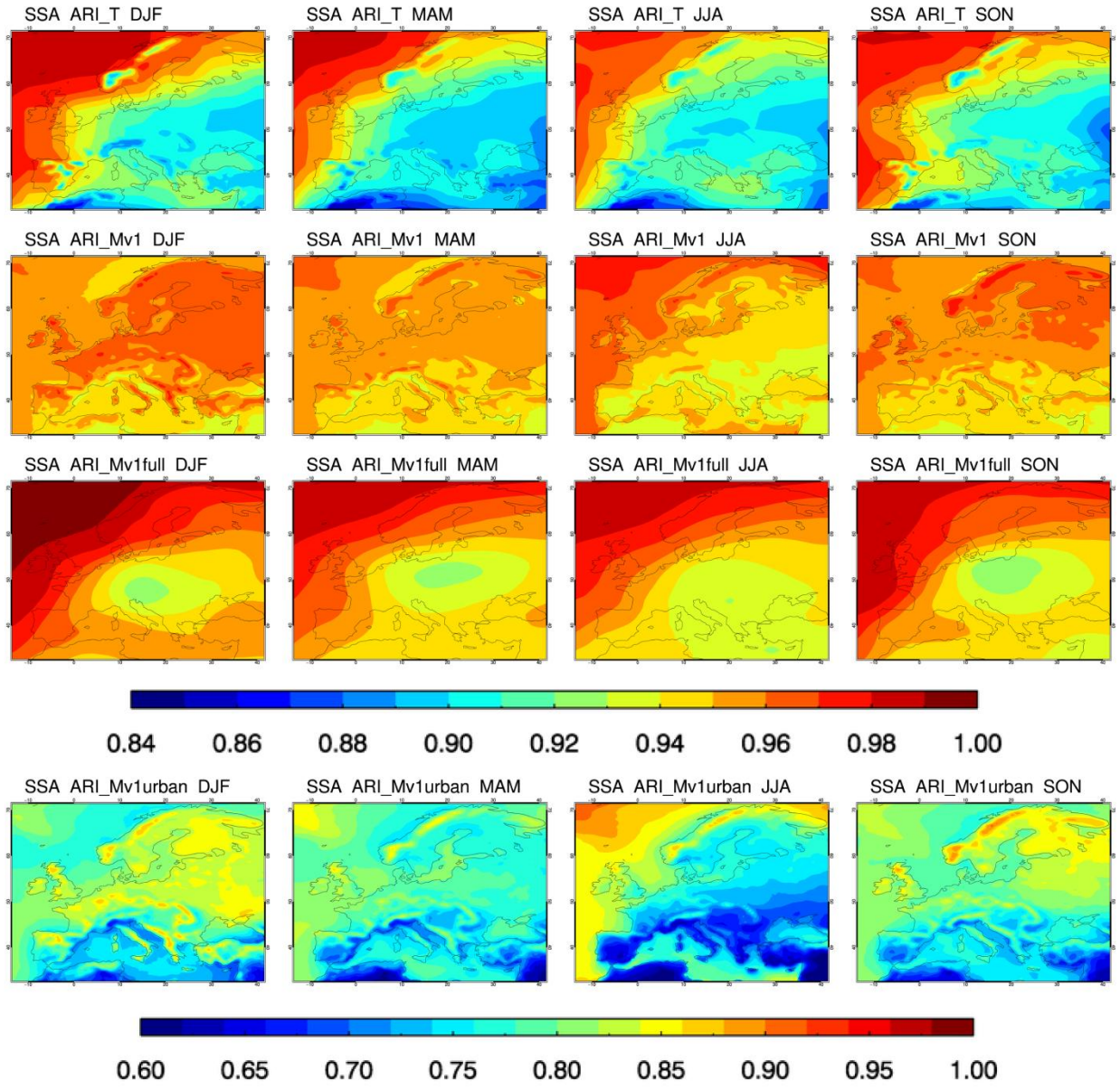


*Figure S1: Single scattering albedo averaged values for the spectral range 0.4-1μm. For simulations ARI_T (aer_opt=1 option), ARI_Mv1 (aer_opt=2 and "rural" aerosol type) and ARI_Mv1full (MAC-v1 SSA climatology). At the bottom row with a different color scale for the ARI_Mv1urban simulation (aer_opt=2 and "urban" aerosol type).*

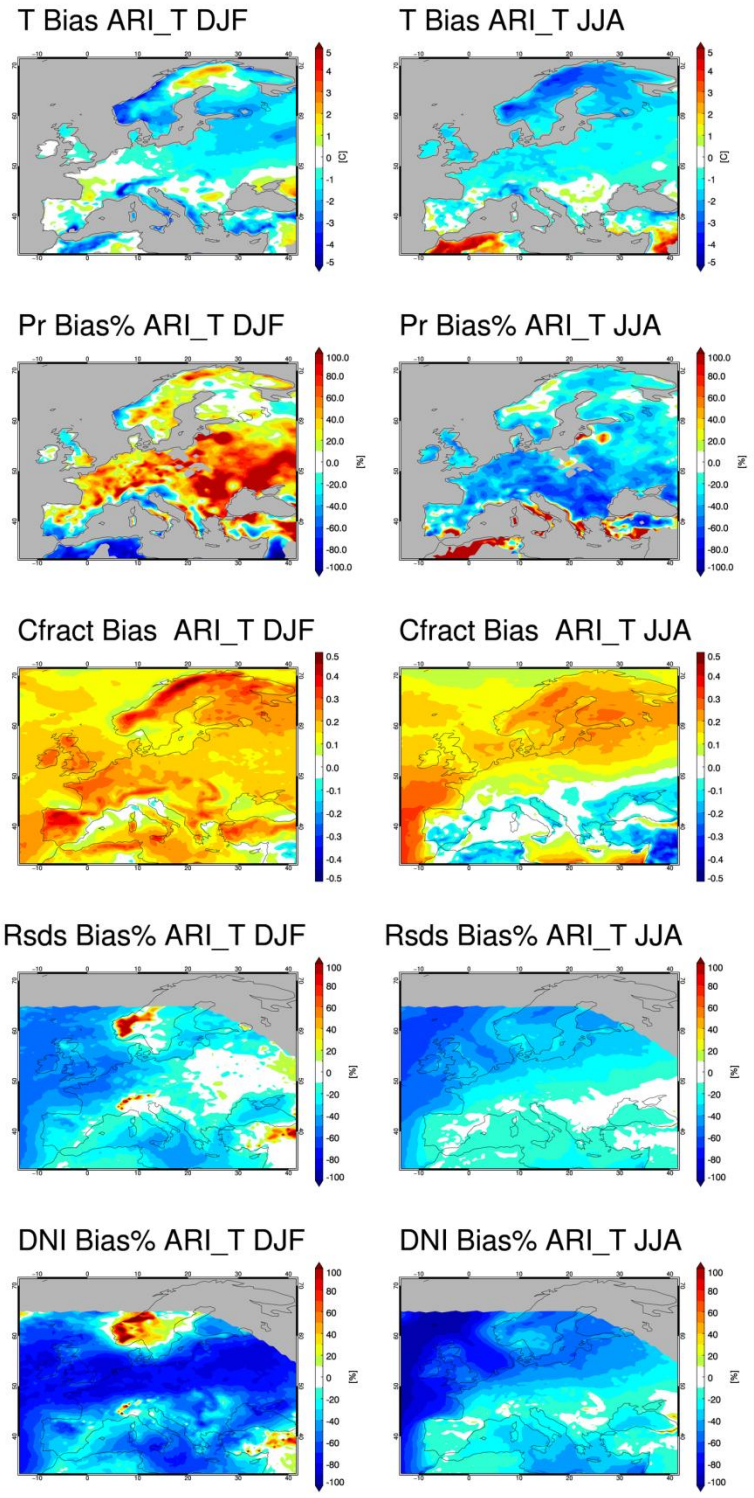


*Figure S2: Bias plots for control simulation ARI_T for winter (DJF-left) and summer (JJA-right). Biases depicted from top to bottom for temperature (T), precipitation (Pr), total cloud fraction (Cfract), down welling shortwave radiation to the surface (Rsds) and direct normalized irradiance at the surface (DNI).*

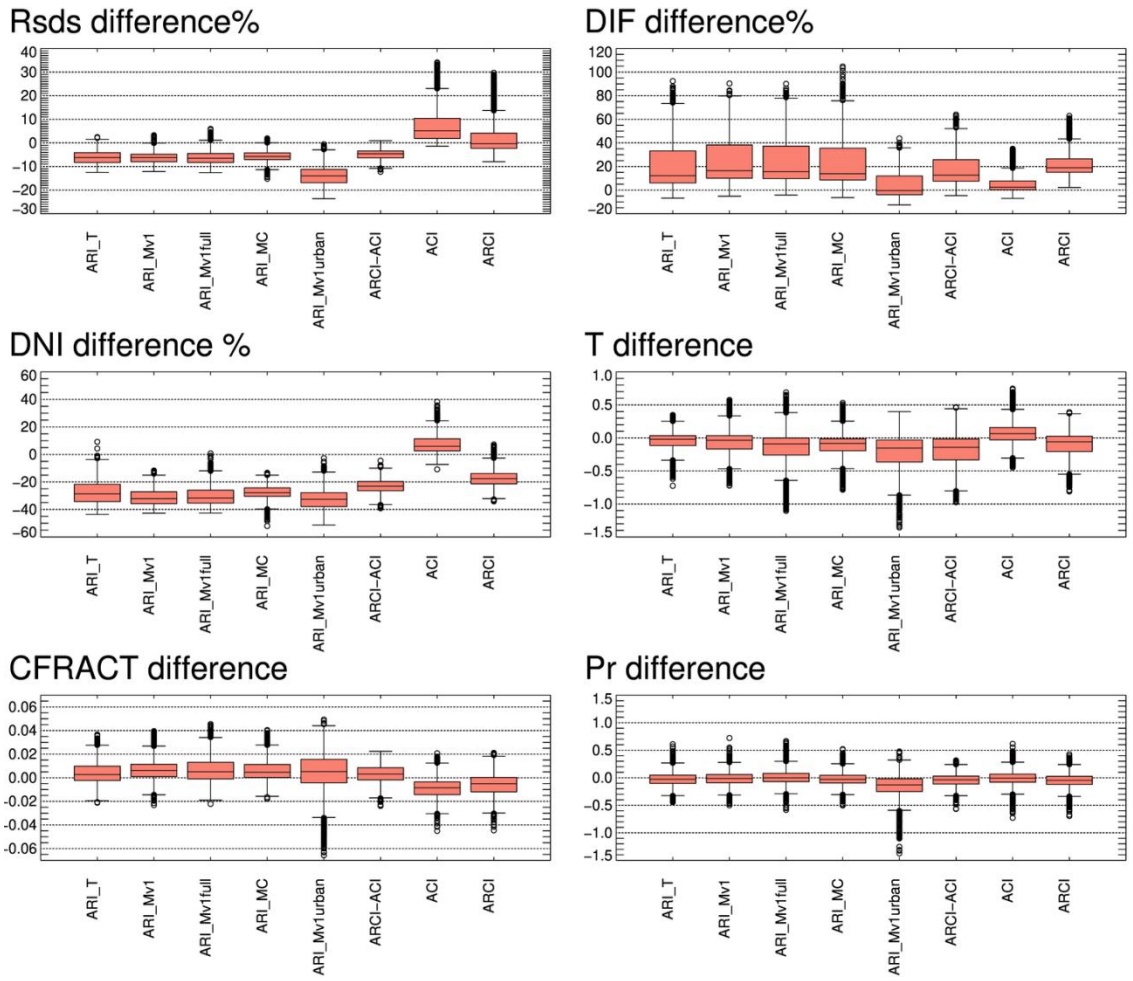


*Figure S3: Plots of differences of the aerosol including simulations from control CON regarding the grid points of the domain on a yearly mean basis. For shortwave radiation at the surface (Rsds), diffuse radiation at the surface (DIF) and direct normalized irradiance (DNI), temperature (T), total cloud fraction CFRACT) and precipitation(Pr). Where stated, the difference of simulation ARCI to ACI is given (ARCI-ACI) to assess the implementation of aerosol-radiation interactions in the Thompson aerosol-cloud interacting cloud microphysics.*

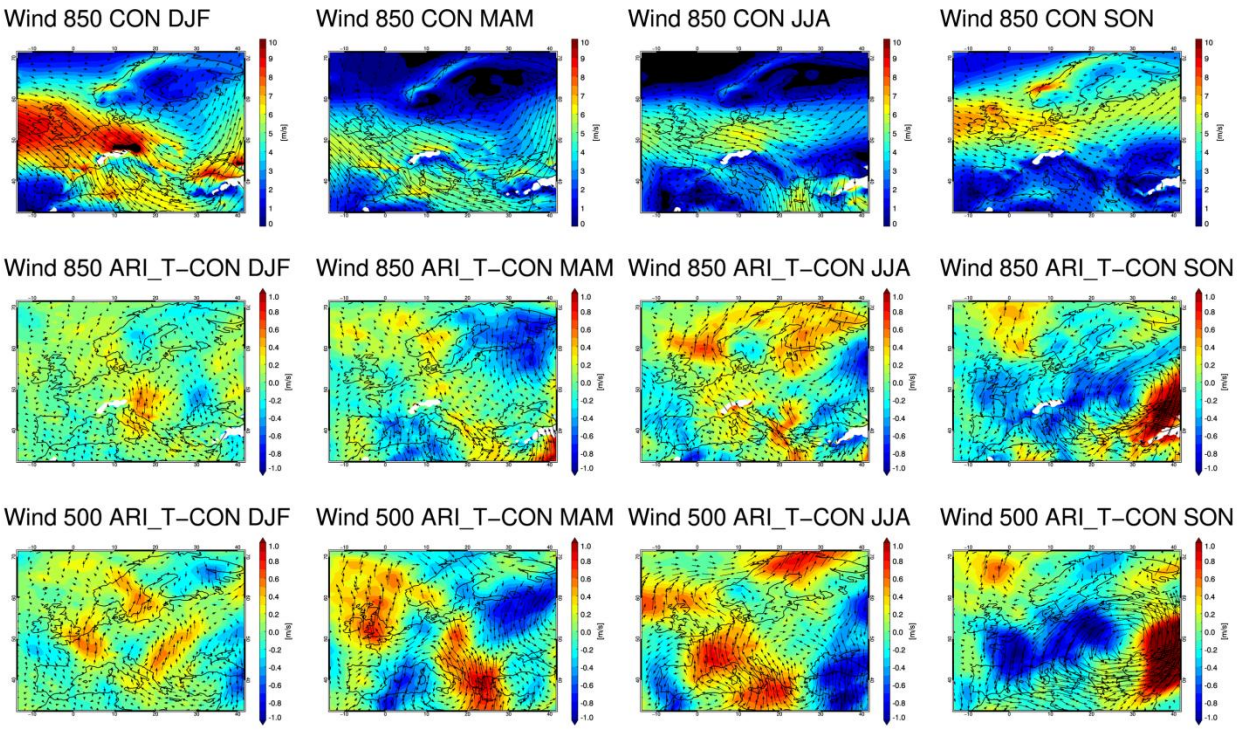


*Figure S4: First row depicts the wind field (arrows) and wind speed (colored contours) of the control experiment for each season. Second row depicts the wind field anomalies (arrows) and meridional wind speed difference (colored contours) of simulation ARI_T from control CON at 850hPa. Likewise for the 500hPa level at the bottom row. Stippling indicates areas where the differences are statistically significant at the 95% level, according to the Mann-Whitney non parametric test.*

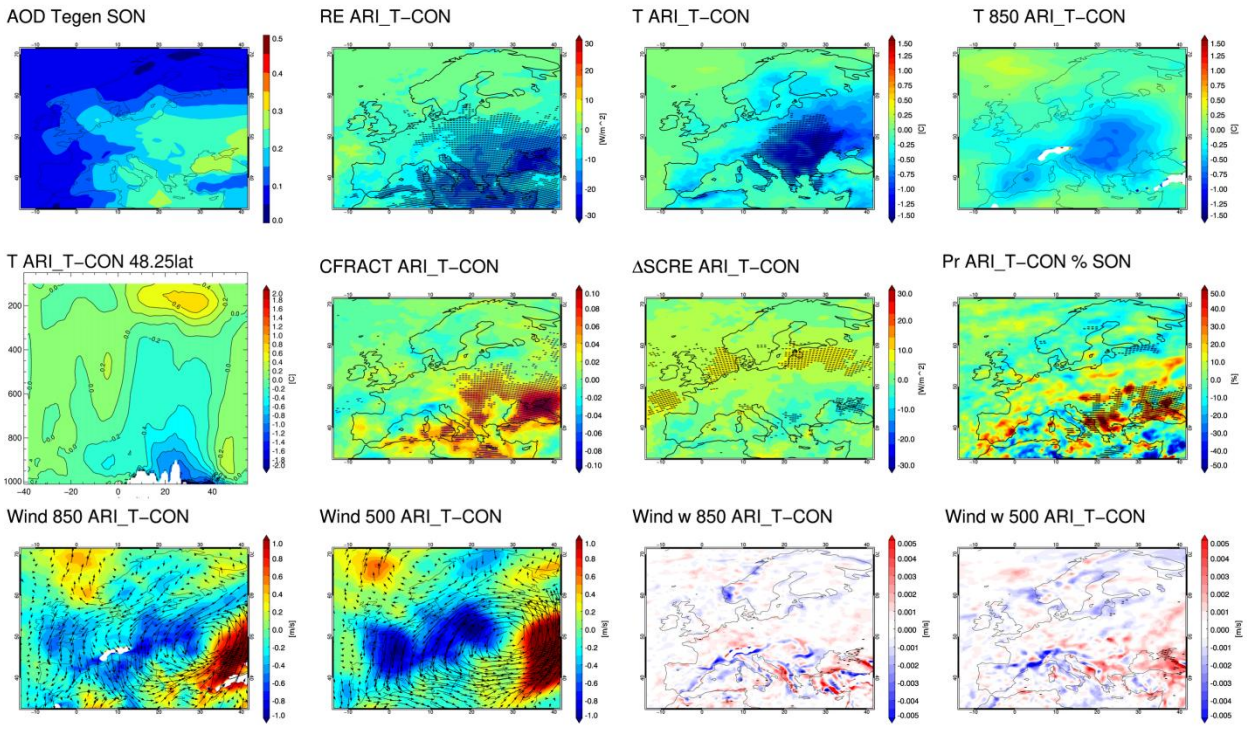


*Figure S.5: Composite analysis for simulation ARI_T in SON. All differences are calculated from CON. Top row, from left to right: AOD field, Radiative forcing RE, difference in near-surface temperature (T), difference in temperature at the 850hPa level (T850). Second row: cross-section at 48.25 latitude depicting differences in temperature vertical profile, difference in cloud fraction (CFRACT), differences in cloud forcing (SCRE), relative (%) difference in precipitation (Pr), Third row: differences in the wind field (arrows) and meridional wind speed (colored contours) at 850hPa, differences in the wind field (arrows) and meridional wind speed (colored contours) at 500hPa, difference in vertical wind speed w at 850hPa and at 500hPa. Stippling indicates areas of statistical significance.*

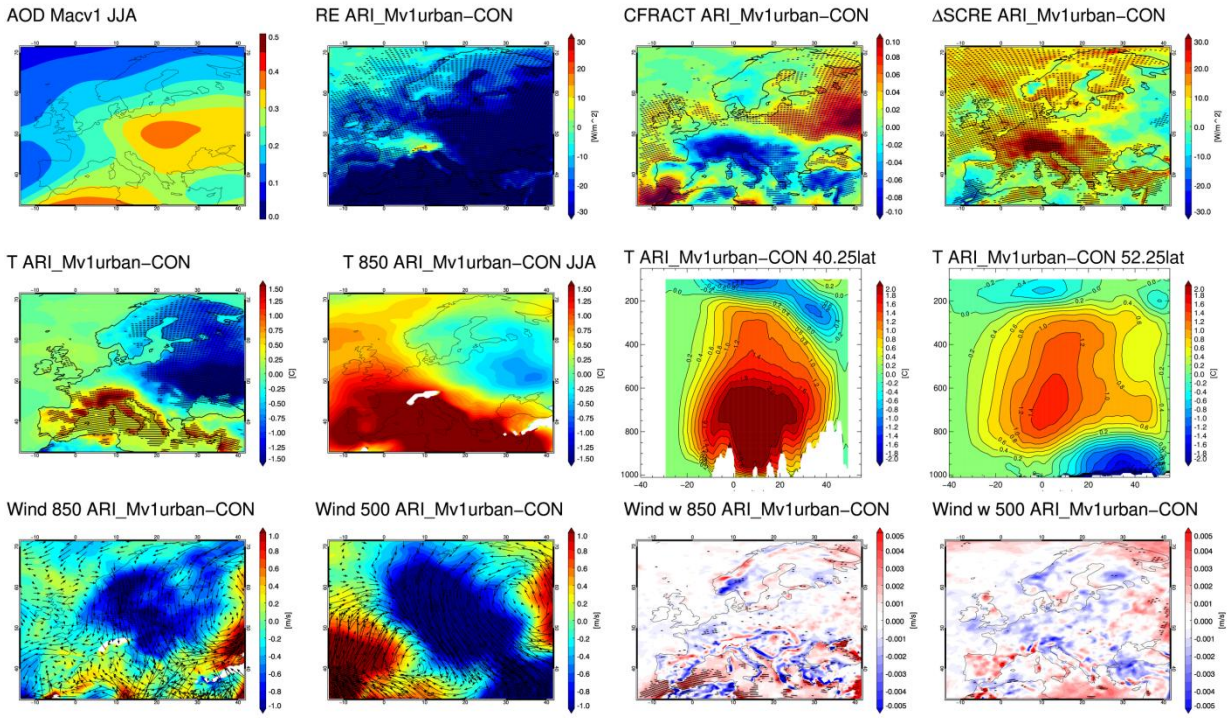


*Figure S6: Composite analysis for simulation ARI_Mv1urban in JJA. All differences are calculated from CON. Top row, from left to right: AOD field, Radiative forcing (RE), difference in cloud fraction (CFRACT), difference in cloud forcing (SCRE). Second row: Difference in near-surface temperature (T), temperature differences at 850hPa (T850), cross-section at 40.25 latitude depicting differences in temperature vertical profile, cross-section at 50.25 latitude depicting differences in temperature vertical profile. Bottom row: difference in the wind field (arrows) and meridional wind speed (colored contours) at 850hPa and 500hPa, difference in vertical wind speed w at 850hPa and at 500hPa. Stippling indicates areas of statistical significance.*

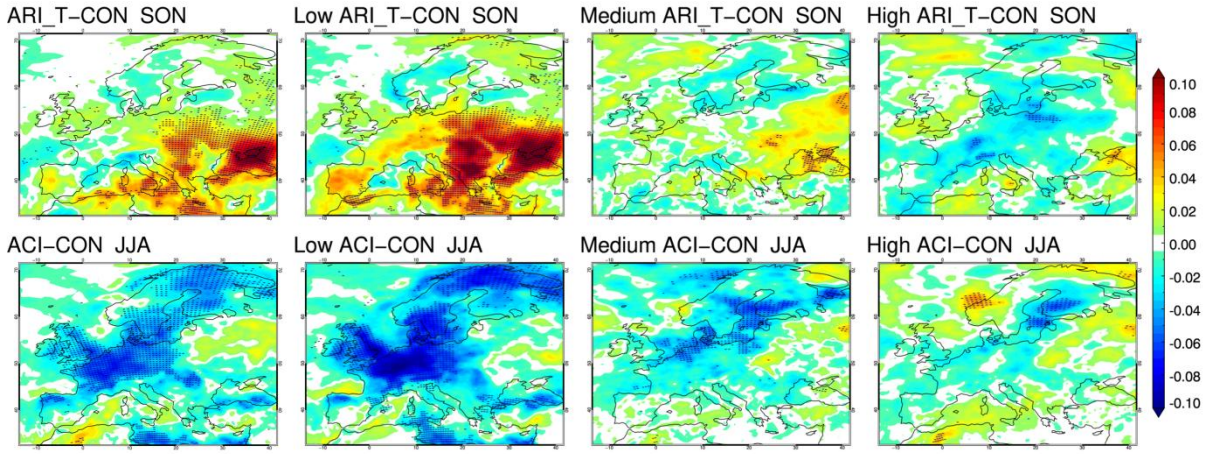


*Figure S.7: Difference from control simulation CON regarding total cloud fraction (first column) as well as cloud fraction for Low, Medium and High clouds (second to fourth column respectively) for simulation ARI_T during Autumn (top row) and simulation ACI during summer (bottom row). Stippling indicates areas where the differences are statistically significant at the 95% level, according to the Mann-Whitney non parametric test.*

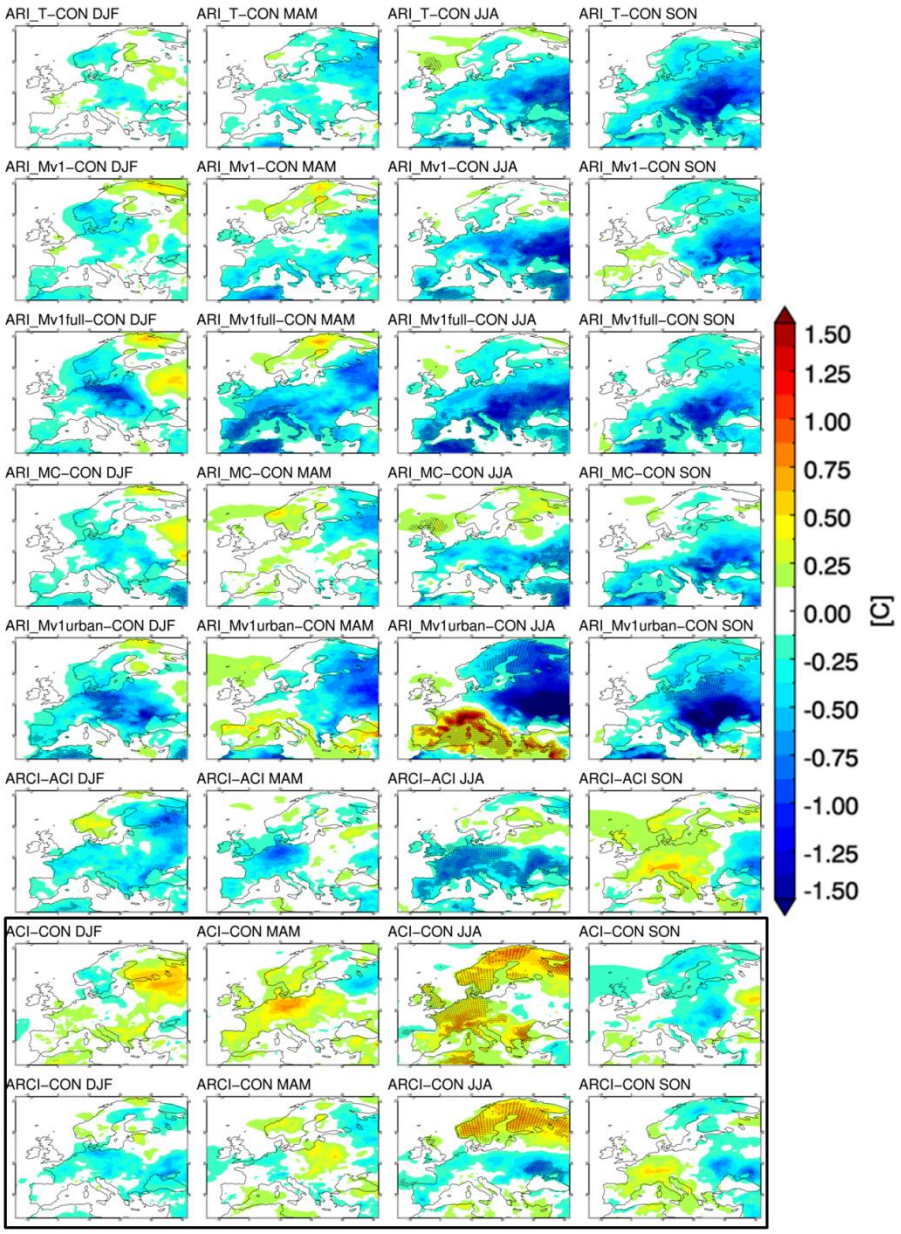


*Figure S8: Near-surface temperature (T) changes from control simulation CON for all experiments and seasons. First five rows present the impact of aerosol-radiation interactions only. Furthermore the temperature difference of ARCI calculated against ACI (ARCI-ACI) is given to assess the implementation of aerosol-radiation interactions in the Thompson aerosol-interacting cloud microphysics (TE2014) that enables aerosol-cloud interactions (row six). Last two rows (black box) present the impact of TE2014 against control CON (row seven, ACI-CON) and TE2014 with aerosol-radiation interactions enabled against control CON (row eight, ARCI-CON). Stippling indicates areas where the differences are statistically significant at the 95% level, according to the Mann-Whitney non parametric test.*

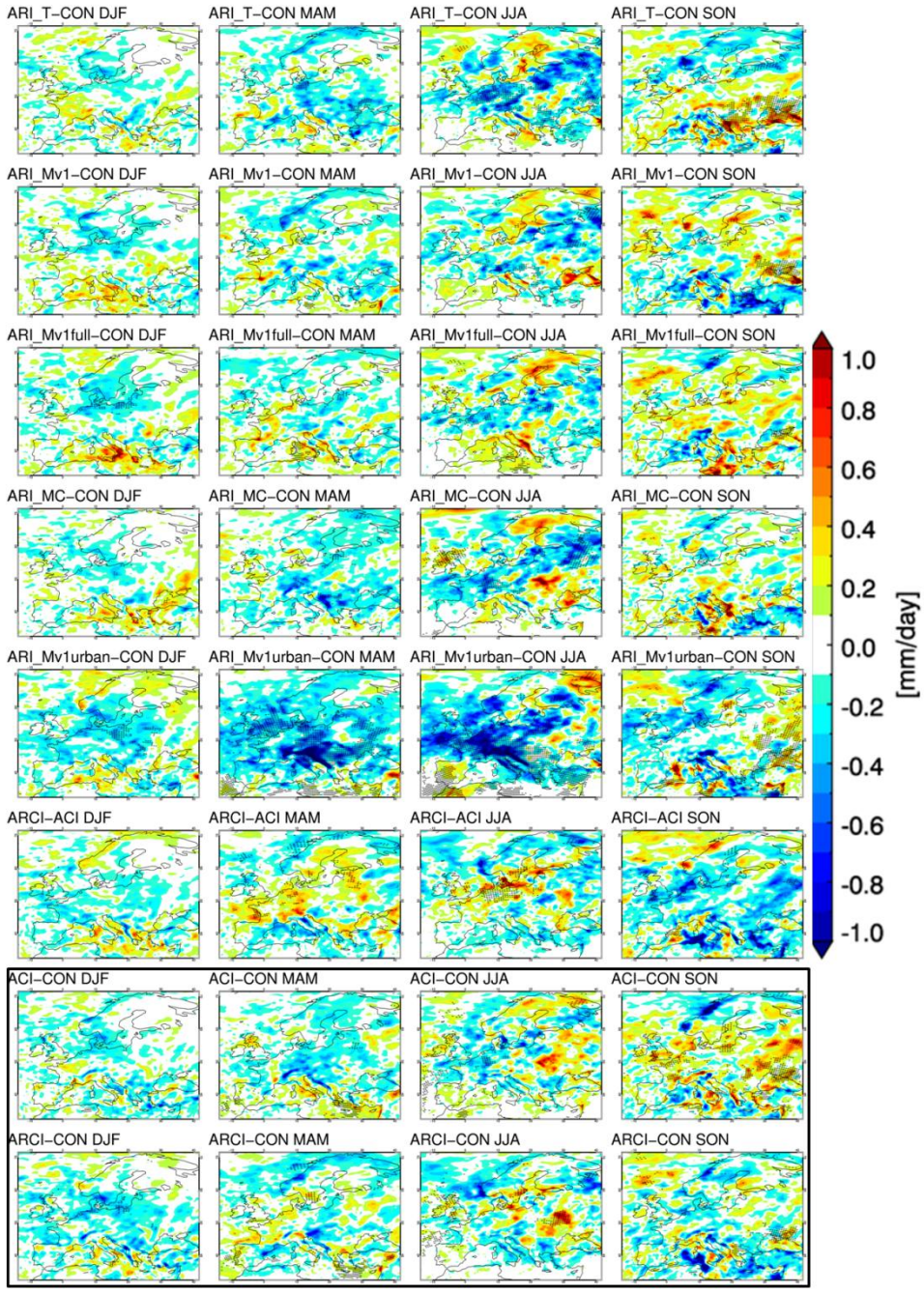


Figure S9: Precipitation difference (mm/day) *from control simulation CON for all experiments and seasons. First five rows present the impact of aerosol-radiation interactions only. Furthermore the temperature difference of ARCI calculated against ACI (ARCI-ACI) is given to assess the implementation of aerosol-radiation interactions in the Thompson aerosol-interacting cloud microphysics (TE2014) that enables aerosol-cloud interactions (row six). Last two rows (black box) present the impact of TE2014 against control CON (row seven, ACI-CON) and TE2014 with aerosol-radiation interactions enabled against control CON (row eight, ARCI-CON). Stippling indicates areas where the differences are statistically significant at the 95% level, according to the Mann-Whitney non parametric test.*